Hindawi
Advances in Civil Engineering
Volume 2021, Article ID 8842077, 13 pages
https://doi.org/10.1155/2021/8842077

Research Article

Investigation of Permanent Deformation Behavior of Steel Slag Asphalt Mixture under Indoor Simulation

Minghua Wei,[1] Chao Yang ,[2] Jun Xie,[2] Shan Liu,[3] Fusong Wang,[2] and Lei Zhang[4]

[1]*School of Transportation, Wuhan University of Technology, Wuhan 430070, China*
[2]*State Key Laboratory of Silicate Materials for Architectures, Wuhan University of Technology, Wuhan 430070, China*
[3]*School of Architecture and Urban Planning, Shandong Jianzhu University, Jinan 250101, China*
[4]*Department of Civil and Environmental Engineering, Norwegian University of Science and Technology, Trondheim 7491, Norway*

Correspondence should be addressed to Chao Yang; hbyangc@whut.edu.cn

Received 28 August 2020; Revised 25 September 2020; Accepted 17 May 2021; Published 27 May 2021

Academic Editor: Timothy O. Olawumi

Previous studies have indicated that steel slag can be used as a substitute for natural aggregates in asphalt mixture, while little attention has been paid to systematic investigation of the influences of various external environmental factors on deformation resistance of steel slag asphalt mixture. In order to understand the service behavior of steel slag asphalt mixture, its permanent deformation under different condition was investigated based on an indoor simulation test. The chemical composition, microscopic structure, surface texture, and volume stability of steel slag were firstly characterized. The uniaxial repeated loading test and standard wheel-tracking test were applied to evaluate the effect of temperature, stress levels, and water damage on the permanent deformation of AC-16 and AC-20 steel slag asphalt mixtures. The results indicate that a higher content of alkaline oxide and high-grade texture index existing in steel slag contribute to its strong absorptivity and adhesion of asphalt. The steel slag demonstrates fine volume stability due to its lower free-CaO (f-CaO) content, autoclave chalked ratio, and immersion expansion ratio. The permanent deformation of steel slag asphalt mixtures increases rapidly under higher stress and temperatures in contrast to lower increment at lower stress and temperatures. Asphalt mixtures at higher stress and higher temperatures and water condition exhibit larger rutting deformation and inferior rutting resistance. AC-16 steel slag asphalt mixture has superior resistance to permanent deformation than AC-20 asphalt mixture. Rutting factors show different degrees of impact in a decreasing order of temperature, water damage, and stress levels. The findings have significant implications for providing a theoretical basis for reusing steel slag in pavement construction and facilitating engineering application of steel slag asphalt mixture.

1. Introduction

Asphalt pavement during service life is prone to crack and damage due to heavy load, overload, high temperature, and water erosion, resulting in rutting disease and affecting its driving comfort and safety [1, 2]. Then, the further development of rutting will also cause other diseases such as network cracks and pits, which will seriously reduce the structural performance and service performance of asphalt pavement [3, 4]. Therefore, the characterization of permanent deformation of hot-mix asphalt mixture becomes currently a research hotspot.

Causing factors of permanent deformation of asphalt mixture were divided into internal factors and external factors [5, 6]. The internal reasons mainly included the properties of asphalt, aggregate, gradation composition, and asphalt-aggregate ratio [7]. The external elements mainly referred to repeated vehicle loads, temperature, and rainwater [8]. Evaluation method of the permanent deformation of asphalt mixture focused on wheel-tracking test, uniaxial repeated loading test, and static loading test [9, 10]. Wheel-tracking test and uniaxial repeated loading test demonstrated better correlations between simulation results of rutting development and field performance, so they were commonly applied to characterize the permanent deformation of asphalt mixture [11, 12].

With regard to the wheel-tracking test, the three-stage model evaluation method has become one of the criteria for

assessing rutting performance of asphalt mixture, which enabled accurate simulation of identification of the transitional points of the rutting phases [13, 14]. Li et al. [15] employed an advanced repeated load permanent deformation (ARLPD) test to investigate the rutting resistance of asphalt pavements, and they found that laboratory results and long-term pavement performance data demonstrated better coincidence, which validated the repeatability of the ARLPD test. The effect of confinement, moisture, stress, and temperature on the three-stage rutting behavior of asphalt mixtures was conducted by Fang et al. [16]. The results indicated that a higher primary rutting rate implied a lower flow number (FN) and faster failure rate. And temperature had the largest impact on rutting followed by water and stress. Multistress loading influence on rutting performance of asphalt mixtures was discussed based on wheel-tracking testing by Javilla et al. [17]. The results showed that lighter stresses applied after overloading stress led to the least damage of mixtures. A multisequenced repeated load (MSRL) test with a fixed number of repeated loads in each sequence was also used to characterize the permanent deformation behavior of asphalt mixture [13]. The conclusions stated that the average strain rate demonstrated nonlinear growth as the stress level increased. Yu et al. [11] proposed the indicators called FN index, accumulated strain to differentiate the impacts of several factors, and found that FN index was suitable for representing the high-temperature performances of asphalt mixtures.

Recently, multiple efforts have been undertaken to improve the resistance to permanent deformation of asphalt mixture. Asphalt modifiers have been introduced, which becomes a widespread and fundamental method. 5% of SBS polymer had a better effect on the improvement of compactibility and permanent deformation resistance according to Khodaii's research [18]. The nonmetallic mineral, like diatomite [19] and steel slag filler [20], was also conducted to enhance the resistance of permanent deformation and moisture for asphalt mixtures. Another feasible approach referred to as asphalt mixtures prepared with an alternative aggregate of steel slag has been involved [21]. As a coproduct of the production of iron and steel, steel slag caused increasing pressure on land occupation and dump fees due to its enormous output and lower utilization rate [22]. Obviously, recycling of steel slag in asphalt mixture was a promising scheme for conserving natural resources and reducing environmental pollution [23]. Research results verified that the mechanical performance of steel slags asphalt mixtures displayed better workability, stiffness, and resistance to moisture damage, fatigue cracking, and permanent deformation [24, 25]. Then, compared with traditional asphalt mixture, asphalt mixture incorporating steel slag owned better pavement performance besides environmental friendliness [26–28]. One concern was considered; the volume stability of steel slag would weaken its performance, while previous studies had concluded that steel slag exhibited fine volume stability due to its lower expansion rate meeting the specification requirements [29–31]. Steel slag asphalt mixture fabricated by the Superpave Gyratory Compactor (SGC) showed various indexes meeting the road performance and superior resistance to permanent deformation than asphalt mixture produced by natural aggregate [32]. Universal Test Machine- (UTM-) 25 had been conducted to investigate permanent deformation behavior of asphalt mixture with steel slag; results showed that its permanent deformation was relatively sensitive to temperature and it can be perfectly simulated with proper equation models. Meanwhile, images and equation models verified that strain per load cycle of specimens was responsible for shear failure of the mixture instead of accumulated permanent strain [33].

However, from the perspectives of the existing literature, it can be inferred that steel slag asphalt mixtures demonstrated excellent resistance to permanent deformation, while little attention has been paid to systematic investigation of the influences of various external environmental factors on its permanent deformation. Therefore, the overall objective of this study is to obtain the permanent deformation behavior of steel slag asphalt mixture under different environment variables. Firstly, X-ray Fluorescence (XRF), Scanning Electron Microscope (SEM), scanning probe microscope, and Aggregate Image Measurement System (AIMS) were employed to evaluate the characteristics of steel slag. Then, volume stability of steel slag, including the content of f-CaO, autoclave chalked ratio, and immersion expansion ratio, was also investigated. Finally, the permanent deformation of steel slag asphalt mixture under different temperature and stress levels and water condition was analyzed.

2. Materials and Methods

2.1. Materials. Base asphalt with 80/100 penetration was obtained from Inner Mongolia, China. The properties of asphalt were presented in Table 1. Steel slag and basalt were provided by ironworks of Baotou in Inner Mongolia and Hubei province, China, respectively. Table 2 listed the basic properties of steel slag and basalt. From the results of crushed stone value and weared stone value, it can be seen that steel slag exhibits higher hardness and better wear resistance and antislip.

2.2. Experimental Methods. Figure 1 shows the flowchart of this research. First, chemical composition, microscopic structure, surface texture, and volume stability of steel slag were characterized. Second, asphalt mixture containing steel slag with two gradations was prepared. Finally, the effect of various external environmental factors on the permanent deformation of steel slag asphalt mixture was determined.

2.2.1. Material Characteristics of Steel Slag. The chemical composition and surface characteristics of steel slag were tested by Axios XRF and JSM-IT300 SEM, respectively. Nanoscope IV Atomic Force Microscope (AFM) was used to evaluate the surface texture of the sample. AFA2 AIMS was applied to acquire the texture index of the sample with a particle size of 9.5–13.2 mm. Texture index is the arithmetic

Table 1: Basic performance indicators of asphalt.

Indexes	Measured values	Specification
Specific gravity	1.032	ASTM D70
Penetration at 25°C (0.1 mm)	89	ASTM D5
Ductility, 5 cm/min, 15°C (cm)	>150	ASTM D113
Softening point (°C)	46	ASTM D36
Apparent viscosity, 135°C (Pa·s)	0.36	ASTM D4402

Table 2: Basic properties of steel slag and basalt.

Materials	Indexes		Measured values	Specification used
Steel slag	Apparent specific gravity	16–19 mm	3.742	ASTM C127
		9.5–16 mm	3.646	
		4.75–9.5 mm	3.602	
		2.36–4.75 mm	3.573	
	Water absorption (%)	16–19 mm	0.51	
		9.5–16 mm	1.49	
		4.75–9.5 mm	1.87	
		2.36–4.75 mm	2.81	
	Crushed stone value (%)		10.3	T0316-2005
	Weared stone value (%)		8.5	T0317-2005
Basalt	Apparent specific gravity	0–2.36 mm	2.838	ASTM C127
	Water absorption (%)		2.92	

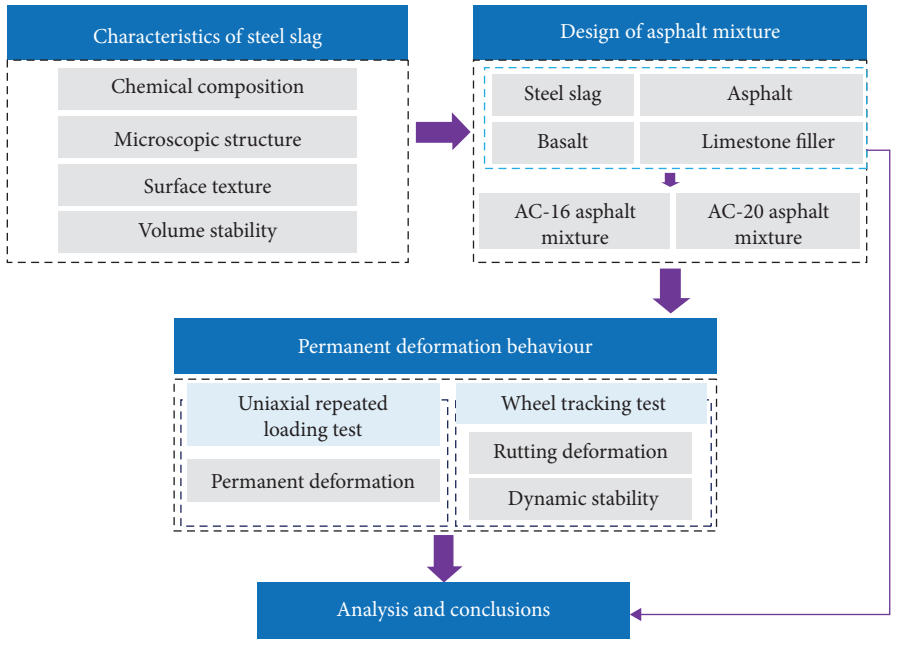

Figure 1: Research flowchart.

mean of the squared values of the stacking detail coefficient, which can be calculated according to the following equation:

$$\mathrm{TI} = \frac{1}{3N}\sum_{i=1}^{3}\sum_{J=1}^{N}\left(D_{i,j}(x,y)\right)^2, \quad (1)$$

where N is the total number of specific coefficients in image analysis; i takes a value of 1, 2, or 3, corresponding to the analysis of horizontal, vertical, and diagonal surface texture; j is the wavelet coefficient index; and (x, y) is the corresponding coordinates of corresponding coefficients in the transformation domain.

The volume stability of steel slag had a great influence on the performance of its mixture [34]. In this study, the content of f-CaO, autoclave chalked ratio, and immersion expansion ratio were used to investigate the volume stability of steel slag. The content of free-CaO was tested through the dissolution-titration method and it can be calculated by (2).

Glycerol-absolute ethanol and benzoic acid-absolute ethanol were used as a solvent for sample and standard titration solution, respectively.

$$\text{f} - \text{CaO}\% = \frac{T_{CaO} \times V}{10 \times G}, \quad (2)$$

where T_{CaO} is milligrams of calcium oxide per milliliter of benzoic acid standard solution (mg/ml); V is the total volume of benzoic acid-absolute ethanol (mL); and G is the weight of the sample (g).

Autoclave chalked ratio was the ratio of the mass of the steel slag less than 1.18 mm after pulverization under the specified pressure and time [35]. Approximately 800 g of samples (particle sizes of 2.36–4.75 mm, 4.75–9.5 mm, 9.5–16 mm, and 16–19 mm) was treated through Y2F-2A autoclave kettle, as shown in Figure 2(b). The saturated steam pressure was 2 MPa and the processing time was 3h. The values of the dial indicator before and after immersion in water can be obtained through the testing device as shown in Figure 2(c). The immersion expansion ratio was acquired by the ratio of the difference value between the two and the original height of the specimen (120 mm in this study) obtained through a heavy compaction experiment. Steel slags with a particle size of 0–31.5 mm were used in this test. The immersion temperature and time were 90°C and 6 h, respectively.

2.2.2. Preparation of Asphalt Mixture. AC-16 (nominal maximum size 16 mm) and AC-20 (nominal maximum size 19 mm) asphalt mixtures were prepared with 4.5% and 4.4% asphalt-aggregate ratio according to the Marshall design method, respectively. Steel slag with a size of 2.36–19 mm and basalt with a size of 0–2.36 mm were used in the two asphalt mixtures based on an equal volume substitution method. The gradation curve of mixtures is shown in Figure 3. Table 3 listed the basic properties of AC-16 and AC-20 asphalt mixtures.

2.2.3. Permanent Deformation Behavior Evaluation of Asphalt Mixture. To better understand the permanent deformation behavior of asphalt mixture, uniaxial repeated loading test and wheel-tracking test were applied to simulate its service characteristics under various external environmental factors. The uniaxial repeated loading test was conducted by UTM-25 (Figure 4) from Australia, which can be applied to simulate the effect of applied loading cycles on rutting development. A cylindrical specimen with a diameter of 100 mm and a height of 100 mm was used in this experiment. And the specimens should be put at the designed temperatures for at least 4 h under a dry atmosphere. A haversine compression loading pulse at 1 Hz was applied in the form of 0.1 s loading period and 0.9 s rest period. Four stress levels (increasing from 0.3 MPa to 0.6 MPa with an interval of 0.1 MPa) and three temperatures (40°C, 50°C, and 60°C) were preset.

The standard wheel-tracking test (WTT) was currently conducted to evaluate the rutting resistance of asphalt mixtures. A square slab specimen with a size of $300 \times 300 \times 50$ mm was prepared according to the Chinese specification. The rolling speed of the wheel was 42 times/min. The applied stresses ranged from 0.5 MPa to 0.9 MPa with an interval of 0.2 MPa and three high temperatures (50°C, 60°C, and 70°C) and water condition were selected as experiment variables.

3. Results and Discussion

3.1. Characteristics of Steel Slag

3.1.1. Chemical Components. Table 4 shows the XRF results of steel slag and basalt. It can be inferred that the chemical composition of steel slags mainly contains CaO, SiO_2, and Fe_2O_3, which accounts for approximately 80% of the total composition, while the highest contents of basalt are SiO_2, followed by Al_2O_3 and CaO. The composition difference of steel slag and basalt is attributed to the discrepancy in the molding process. For steel slag, oxide cosolvent is required during its production process. Steel slag with higher content of alkaline oxide can neutralize the carboxylic acid in asphalt, resulting in emergence of alkaline salt with strong absorbability. Then, an interface layer transmitting stress between steel slag and asphalt is formed, thus enhancing the adhesion of both of them.

3.1.2. Microscopic Structure and Texture. It can be seen from the SEM images as shown in Figure 5 that steel slag owns a rougher surface than basalt, and its shape is irregular. Steel slag with rich surface textures will increase its effective contact area with asphalt so as to improve its adhesion to asphalt. There are many micropores in steel slag, which make the water absorption rate of steel slag higher and also promote the absorption of asphalt. The surface of steel slag and basalt demonstrates the accumulation phenomenon of tiny dust, which is due to the hydration product of $CaCO_3$ and other minerals in the aggregate.

Figure 5(a) shows the results of the texture index for steel slag and basalt. The texture index of samples can be divided into four levels: low grade (0 to 200), medium grade (200 to 500), high grade (500–750), and very high grade (750–1000). Results in Figure 5(a) show that the texture indexes of steel slags are mainly distributed in the high grade, in contrast with a medium grade for basalt. The average value of texture index for steel slag is 645.8, which is approximately 1.5 times of basalt. Microtexture from AFM result as shown in Figure 6(b) is consistent with the conclusion of the AIMS test. In general, the surface texture and roughness of steel slag are much higher than that of basalt. Researches indicated that aggregate with a higher value of texture index implies richer surface texture and better adsorption capacity to asphalt. It means that the application of steel slag instead of basalt in asphalt mixture can improve its adhesion with asphalt.

3.1.3. Volume Stability. When f-CaO is mixed with water, its molar volume will nearly double, so the content of f-CaO in steel slag directly affects its volume stability. The

Figure 2: Testing device for volume stability of steel slag: (a) contents of f-CaO; (b) autoclave chalked ratio; (c) immersion expansion ratio.

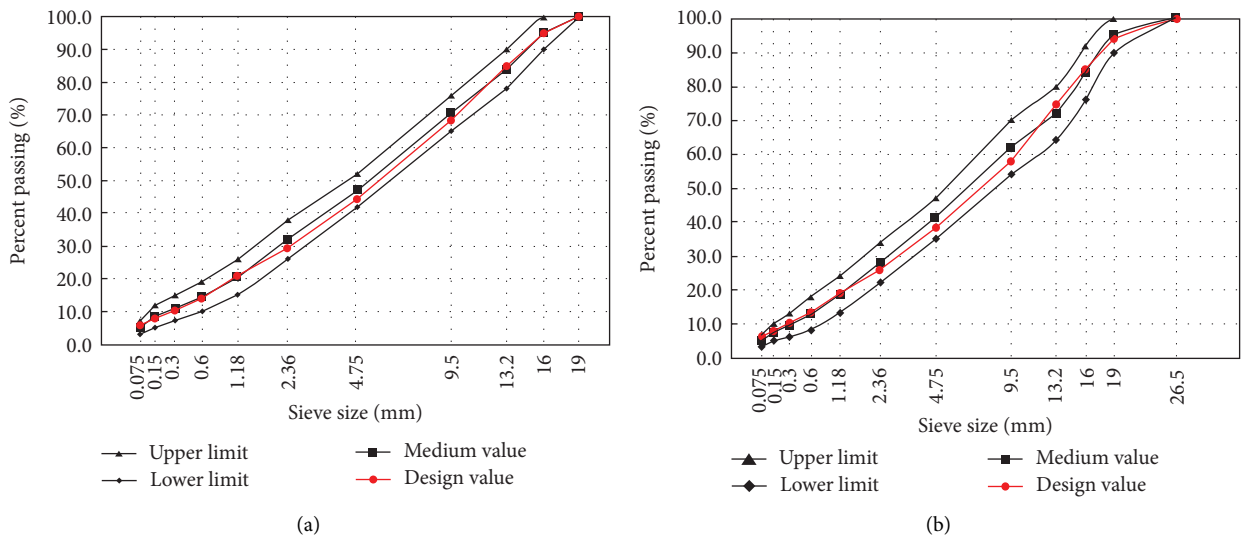

Figure 3: Hybrid mixture gradation of steel slag asphalt mixture (a) AC-16; (b) AC-20.

Table 3: Basic properties of steel slag asphalt mixtures.

Indexes	AC-16	AC-20
Asphalt-aggregate ratio (%)	4.5	4.4
Bulk gravity (g/cm^3)	2.879	2.927
Marshall stability (kN)	21.0	12.5
VMA (%)	14.1	14.2
VFA (%)	71.4	72.3
Residual Marshall stability (%)	94.1	93.8
Tensile strength ratio (%)	91.3	89.1

specification requires that the f-CaO content of steel slag in asphalt mixture should not exceed 3% [36]. Figure 7(a) illustrates the content of f-CaO of steel slag with different particle size. Results exhibit that contents of f-CaO in steel slag are all lower than 2% except sample with a size of 5–10 mm.

The autoclave chalked ratio of steel slag with different particle size is shown in Figure 7(b). With the increased particle size for steel slag, its autoclave chalked ratio decreases obviously. This is ascribed to the fact that the decrease of contact area between steel slag and steam leads to the decrease of their chemical reaction rate. The autoclave chalked ratio of steel slag with different particle sizes is less than 2.5%, which is far lower than the requirement of 5% in the specification [35].

It can be seen from Figure 7(c) that the immersion expansion ratio of steel slag is kept below 1% within 10 days, and the highest value only reaches 0.78%. This meets the requirement that the immersion expansion ratio of steel slag should not exceed 1.8% [36]. It is illustrated that steel slag can be applied in asphalt mixture without special treatment. Figure 7(c) shows that the immersion expansion ratio

(a) (b)

Figure 4: Experimental devices in this study: (a) UTM-25 apparatus for uniaxial repeated loading test; (b) rutting apparatus for wheel-tracking test.

Table 4: Chemical components of steel slag and basalt.

Content (wt%)	Compound						
	CaO	MgO	SiO_2	Al_2O_3	Fe_2O_3	P_2O_5	LOI
Steel slag	45.43	5.96	13.47	2.25	19.43	0.85	1.37
Basalt	7.14	5.59	58.09	18.42	0.53	0.73	1.02

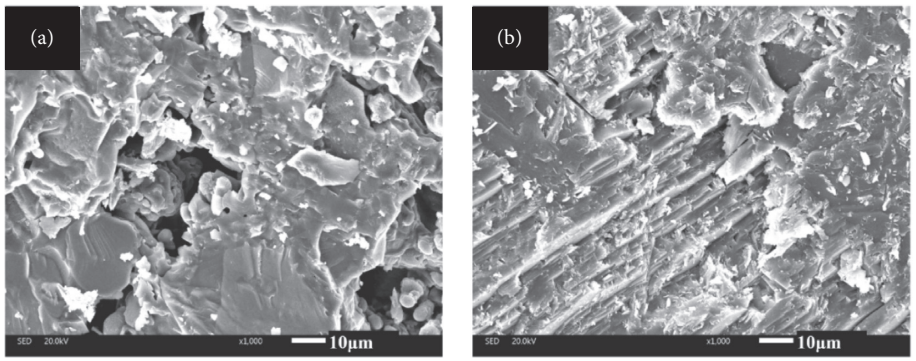

Figure 5: Microscopic structure of steel slag and basalt: (a) steel slag; (b) basalt.

increases gradually with the increase of immersion time. And the increase rate was fast in the first 5 days, gradually increased slowly in the last five days, and tended to be stable at about 0.77% at 8–10 days. This shows that most of f-CaO in steel slag has fully reacted with water within 10 d water bath time. It is concluded that the steel slag exhibits fine volume stability, which can also be verified from the results of f-CaO content and autoclave chalked ratio.

3.2. Permanent Deformation Behavior of Steel Slag Asphalt Mixture

3.2.1. Results of Uniaxial Repeated Loading Test. The permanent deformation of asphalt pavement is divided into three stages. The primary stage is corresponding to the compaction stage, in which the deformation rate of asphalt mixture decreases with the increase of cycle times. This is mainly due to the compaction effect of vehicle load on the pavement and the decrease of pavement layer thickness. The secondary stage is corresponding to the plastic flow stage, in which the deformation rate remains unchanged with the increase of cycle times. Asphalt mixture on both sides of the action point demonstrates the phenomenon of uplift, which is ascribed to transverse shear stress caused by the different loads on the same horizontal surface. Under the tertiary stage-shear failure stage, it mainly shows that the deformation rate increases with the increasing number of cycles. The formation can be explained that the skeleton stability of asphalt pavement decreases and the deformation rate increases exponentially for fatigue crack and rutting.

Figure 8 shows uniaxial repeated permanent deformation of AC-16 and AC-20 steel slag asphalt mixtures under

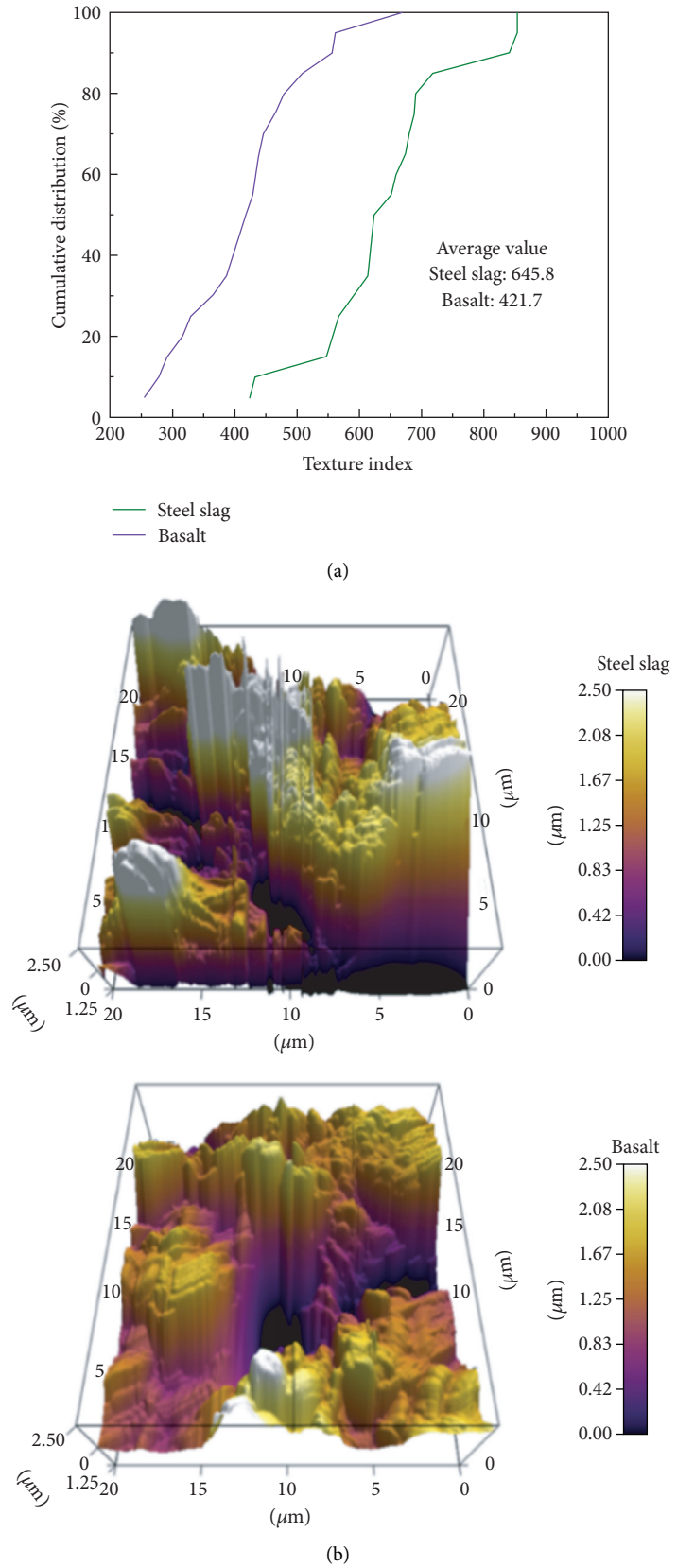

Figure 6: Texture of steel slag and basalt: (a) texture index from AIMS; (b) microtexture from AFM.

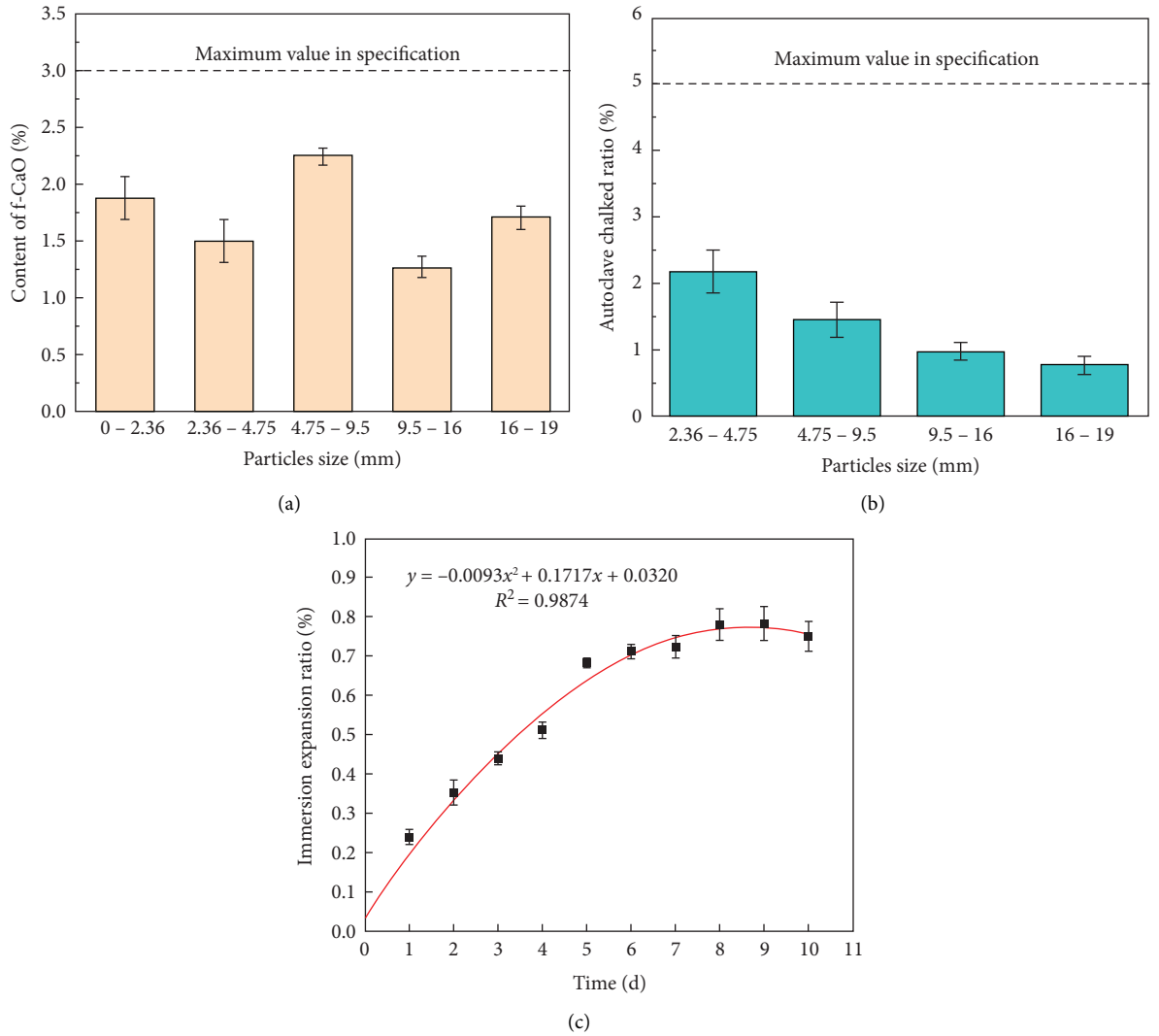

Figure 7: Volume stability of steel slag: (a) content of f-CaO; (b) autoclave chalked ratio; (c) immersion expansion ratio.

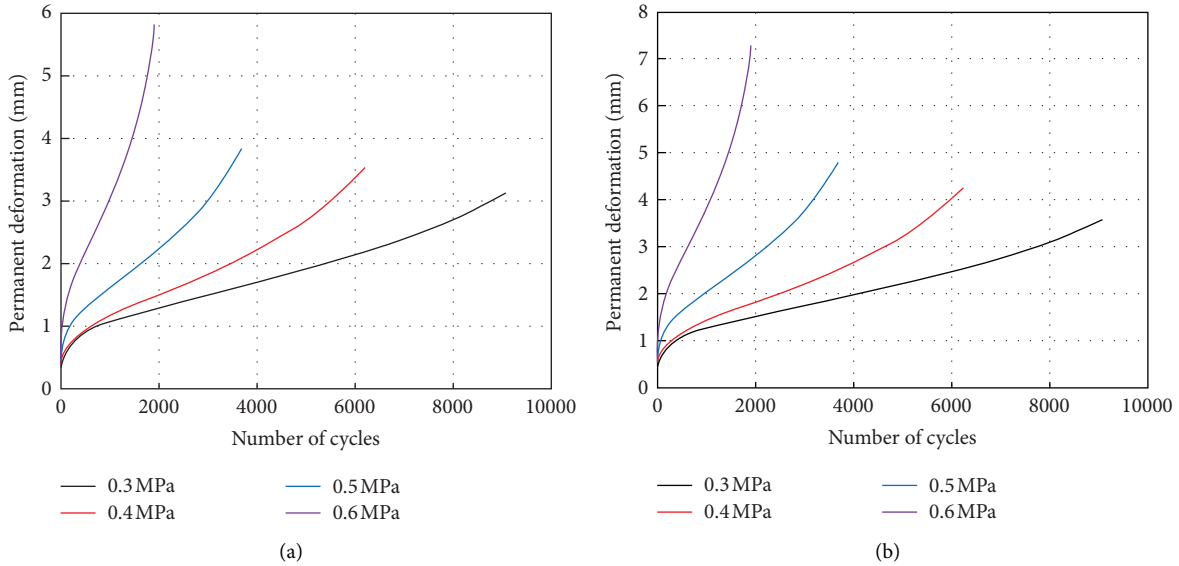

Figure 8: Uniaxial repeated loading test results of steel slag asphalt mixtures under different stress levels (a) AC-16; (b) AC-20.

different stress levels. The experimental constant temperature was 40°C for all samples. It can be seen from Figure 8(a) that the permanent deformation of the AC-16 steel slag asphalt mixture increases with the increase of stress levels. All asphalt mixtures under various stress levels have entered the third stage of permanent deformation, and its permanent deformation rate increases rapidly with the increase of load times under this stage. When the number of cycles reaches 2000, the deformation of asphalt mixtures at 0.3 MPa, 0.4 MPa, and 0.5 MPa is 1.322 mm, 1.519 mm, and 2.250 mm, while for 0.6 MPa, its deformation approaches 6 mm. It is also found that the number of cycles that caused deformation of 3.0 mm of the four stress levels of 0.6 MPa, 0.5 MPa, 0.4 MPa, and 0.3 MPa is 980, 2994, 5518, and 8806, respectively. It can be inferred that permanent deformation of mixtures demonstrates a gentle increasing tendency at low-stress levels (less than 0.5 MPa) with the increase of stress, while it increases rapidly under the high-stress levels stage.

The uniaxial repeated loading test results of the AC-20 steel slag asphalt mixture are shown in Figure 8(b). The general tendency of deformation for AC-20 asphalt mixture is consistent with that of AC-16 asphalt mixture as the variation of stress levels. But deformation for AC-20 asphalt mixture is slightly higher than AC-16 asphalt mixture, which means that it is more inferior to resist permanent deformation. The number of cycles for AC-20 asphalt mixture that caused deformation of 3.0 mm of the four stress levels of 0.6 MPa, 0.5 MPa, 0.4 MPa, and 0.3 MPa is 618, 2227, 4617, and 7770, respectively. The results show that the number of cycles of AC-20 asphalt mixture required to reach the same deformation is less than AC-16 asphalt mixture. It then leads to an assumption that steel slag asphalt mixture with a larger nominal maximum size shows greater permanent deformation.

Figure 9 indicates the uniaxial repeated loading test results of steel slag asphalt mixtures under different temperatures. The constant stress levels of 0.5 MPa were applied in this experiment. The permanent deformation of both AC-16 and AC-20 asphalt mixture increases with increasing experimental temperature. All samples at three temperatures have entered the tertiary stage of permanent deformation. As shown in Figure 9(a), the number of cycles that caused deformation of 3.0 mm of the three temperatures of 40°C, 50°C, and 60°C is 2984, 1732, and 509, respectively. The corresponding number of cycles is 2567, 1363, and 407 for the AC-20 asphalt mixture in Figure 9(b). The fastest shear failure is all observed when the temperature rises to 60°C in two steel slag asphalt mixtures, indicating that they are more inclined to reach the tertiary stage of permanent deformation under higher temperature. The trend of the deformation-cycle curve with a temperature of 40°C or 50°C is gentle, but it turns steeper under 60°C. It is indicated that the deformation of asphalt mixture becomes extremely sensitive to the number of loads at a higher temperature.

3.2.2. Results of Rutting Test. Rutting disease of asphalt pavement is mainly caused by traffic load, temperature, and water damage, which seriously affects the durability of pavement. The WTT, a common evaluation method for rutting resistance of asphalt mixture, is involved in this test with the above three influence factors. Figure 10 exhibits the rutting deformation of steel slag asphalt mixtures at different temperature. The standard stress of 0.7 MPa was selected as the constant load. It can be found from Figure 10(a) that the rutting deformation of asphalt mixture increases with the increase of the number of cycles and temperature. The rutting deformation of AC-16 asphalt mixture with a maximum cycle of 15000 reaches 3.78 mm, 6.16 mm, and 8.39 mm under a temperature of 50°C, 60°C, and 70°C, respectively. When the temperature is 50°C, the rutting deformation of the asphalt mixture is only 3.42 mm with a cycle of 10000, but its deformation increases to 1.7 times and 2.3 times at 60°C and 70°C, respectively.

Rutting deformation of AC-20 asphalt mixture as shown in Figure 10(b) displays that the general variation tendency of the column is consistent with that of AC-20 asphalt mixture. And yet AC-20 asphalt mixture reveals larger rutting deformation than that of AC-16 asphalt mixture. Deformation of asphalt mixture multiplies greatly as temperature increases from 50°C to 70°C.

It is inferred that the rutting deformation of steel slag asphalt mixture is sensitive to the variation of temperature. And AC-20 steel slag asphalt mixture owns inferior resistance to rutting deformation compared with AC-16 asphalt mixture.

Figure 11 indicates the effect of stress on the rutting deformation of steel slag asphalt mixtures. The standard temperature of 60°C was applied. The rutting deformation of AC-16 and AC-20 steel slag asphalt mixtures increases with the increase of stress levels. As shown in Figure 11(a), deformation of AC-16 asphalt mixture with a cycle of 10000 reaches 4.75 mm, 5.82 mm, and 7.94 mm under a temperature of 0.5 MPa, 0.7 MPa, and 0.9 MPa, respectively. When the number of cycles achieves the maximum of 15000, deformation at 0.9 MPa reaches 8.32 mm, which is 1.35 times of standard stress of 0.7 MPa and 1.62 times of 0.5 MPa.

As for the AC-20 steel slag asphalt mixture, its rutting deformation is higher than that of the AC-16 asphalt mixture at the same stress levels and the number of cycles. The deformation of the mixture increases by 1.17 mm with stress increasing from 0.5 MPa to 0.7 MPa, and increment is 3.35 mm when stress is further up to 0.9 MPa. It is concluded that the deformation increases gently with the increase of stress levels under the low-stress stage (less than 0.7 MPa), and it raises sharply with further increasing stress. Compared with Figure 9, it can be found that the sensitivity of deformation to the fluctuation of stress levels is lower than that of temperature.

Figure 12 presents the effect of moisture damage on the rutting deformation of steel slag asphalt mixtures. The standard temperature of 60°C and stress of 0.7 MPa was used in this simulation experiment. It is observed from Figure 12(a) that moisture damage demonstrates no obvious influence on the deformation of AC-16 asphalt mixture when the number of cycles is less than 10000. As the number of cycles further increases, the harmful effect of water conditions on rutting deformation is fully reflected. Rutting

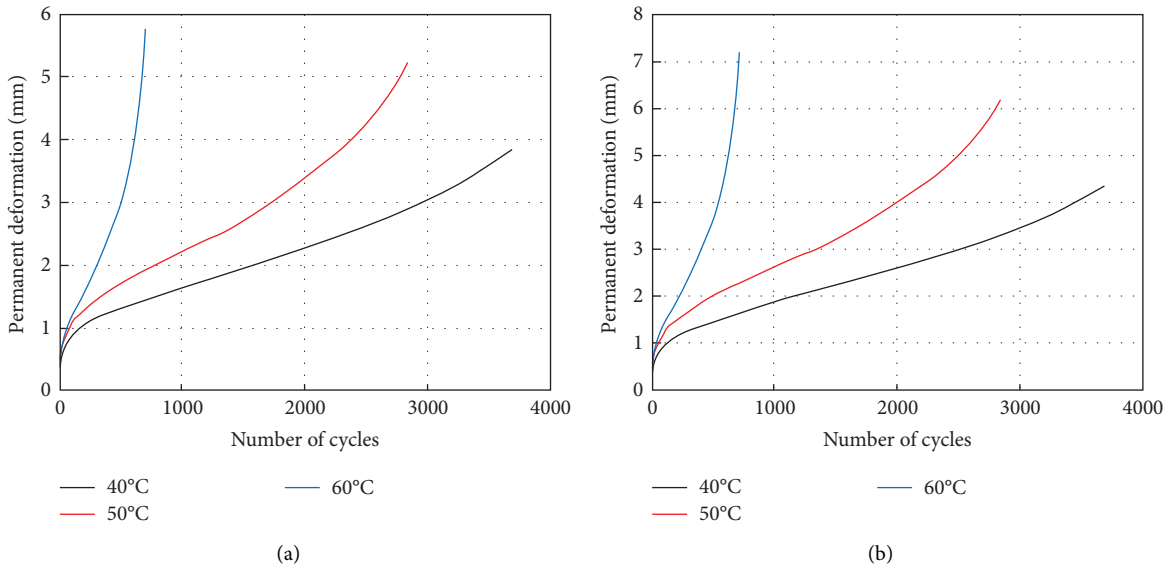

Figure 9: Uniaxial repeated loading test results of steel slag asphalt mixtures under different temperatures (a) AC-16; (b) AC-20.

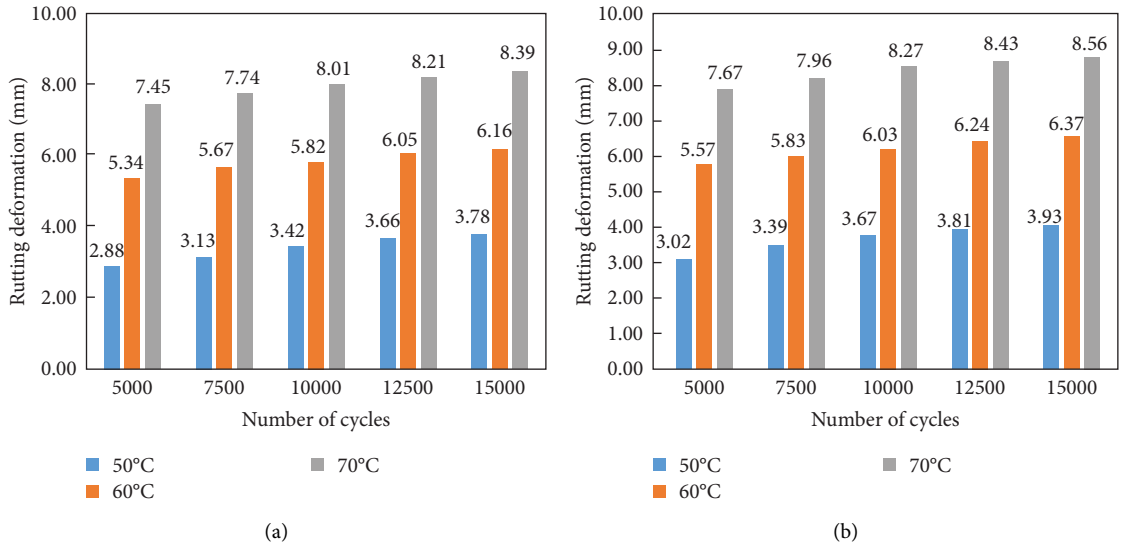

Figure 10: Effect of temperature on the rutting deformation of steel slag asphalt mixtures: (a) AC-16; (b) AC-20.

deformation of asphalt mixture under water condition reaches 12.95 mm with a number cycles of 15000, which is 2.1 times of blank control group. The trend of deformation variation of AC-20 asphalt mixture as shown in Figure 12(b) under moisture damage is similar to that of AC-16 asphalt mixture. For AC-20 asphalt mixture, its rutting deformation under the same number of cycles exceeds AC-16 asphalt mixture, and this conclusion is consistent with analysis results of temperature and stress levels.

In order to evaluate the influence degree of temperature, stress, and water, the dynamic stability index is applied to represent the rutting resistance of steel slag asphalt mixture. The effect of the above three factors on the dynamic stability is discussed based on an orthogonal design experiment as an example of AC-16 steel slag asphalt mixture. The analysis results of asphalt mixture under different variables are shown in Table 5. K and $\overline{x}$ are defined as sum and average of dynamic stability at the same level, respectively. R refers to the range between the maximum and minimum of $\overline{x}$. Table 5 indicates that R (temperature) > R (water) > R (stress) for AC-16 steel slag asphalt mixture. It is inferred that temperature shows the largest impact on the rutting resistance of asphalt mixture, followed by water damage and stress levels. The conclusion is consistent with the research results of the AC-20 limestone asphalt mixture provided by Fang et al. [16].

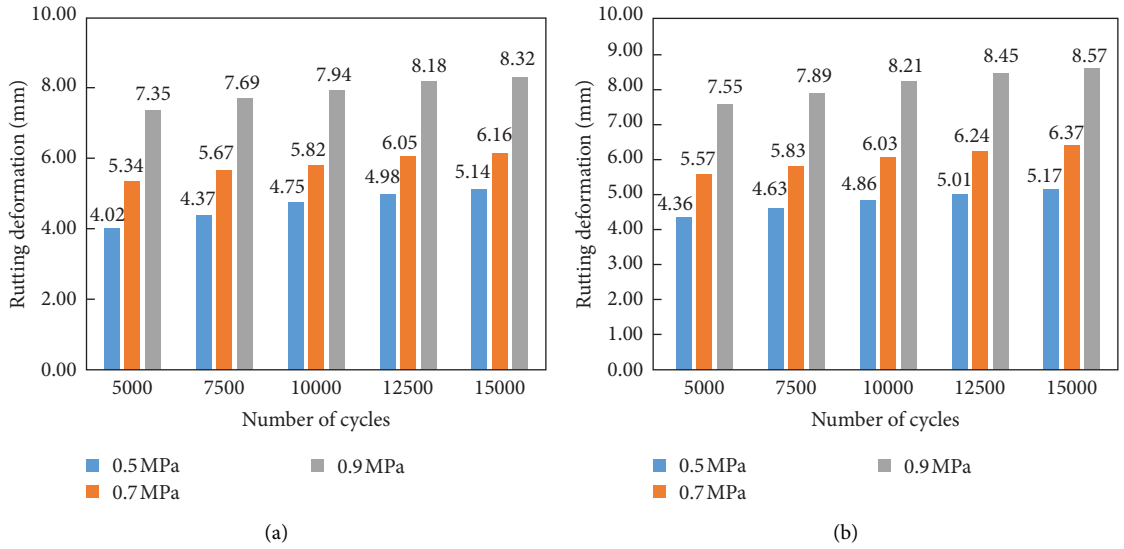

Figure 11: Effect of stress levels on the rutting deformation of steel slag asphalt mixtures: (a) AC-16; (b) AC-20.

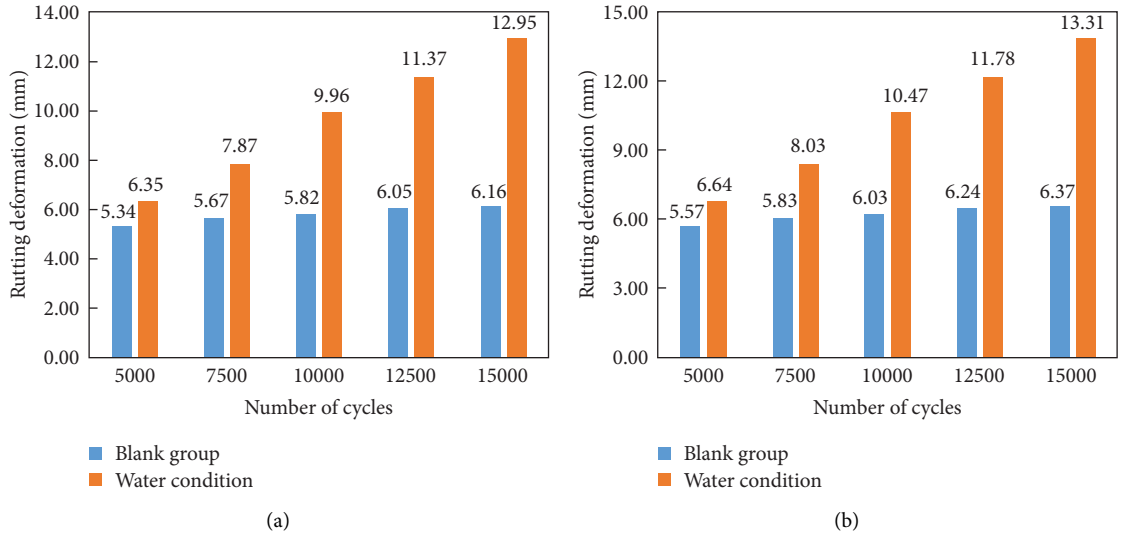

Figure 12: Effect of moisture damage on the rutting deformation of steel slag asphalt mixtures: (a) AC-16; (b) AC-20.

Table 5: Analysis results of dynamic stability for AC-16 steel slag asphalt mixture.

Number	Temperature (°C)	Stress (MPa)	Wet or dry	Dynamic stability (times/mm)
1	50	0.5	Wet	1625
2	50	0.7	Wet	1163
3	50	0.9	Dry	1747
4	60	0.5	Dry	2274
5	60	0.7	Wet	1058
6	60	0.9	Wet	876
7	70	0.5	Wet	806
8	70	0.7	Dry	1089
9	70	0.9	Wet	131
K_1	4535	4705	5110	
K_2	4208	3310	2845	
K_3	2026	2754	2814	
$\overline{x}_1$	1512	1568	1703	
$\overline{x}_2$	1403	1103	948	
$\overline{x}_3$	675	918	938	
R_j	836	650	765	

4. Conclusions

This work investigated the characteristics of steel slag, including chemical composition, microscopic structure, surface texture, and volume stability. The influence of temperature, stress levels, and water damage on the permanent deformation of steel slag asphalt mixtures was also discussed. Based on the above results, the following conclusions can be obtained:

(1) Steel slag displays higher content of alkaline oxide and average texture index than basalt. The content of f-CaO and autoclave chalked ratio are far less than the maximum requirements in the specification and immersion expansion ratio is kept below 1% within 10 days for steel slag, indicating its fine volume stability.

(2) The permanent deformation of steel slag asphalt mixtures demonstrates a gentle increasing tendency with an increase in the number of cycles at low stress and temperature, while it rises rapidly at higher stress and temperature. Steel slag asphalt mixture displays larger rutting deformation under higher stress and higher temperatures and water condition, which means its inferior rutting resistance. AC-16 steel slag asphalt mixture reveals superior resistance to permanent deformation compared with AC-20 asphalt mixture.

(3) Results of dynamic stability illustrate that temperature exhibits the largest influence on the rutting resistance of steel slag asphalt mixture due to its maximum range, followed by water damage and stress levels. It is consistent with the established knowledge about asphalt mixture prepared with natural aggregate.

(4) Asphalt mixture with coarse aggregate of steel slag shows nonexistence of poor volume stability, while it exhibits fine ability to resist permanent deformation conversely. So the application of steel slag in the upper and middle surface of asphalt pavement becomes a better scheme that contributes to the sustainable development and cleaner pavement construction for road engineering.

Data Availability

All the data generated or analyzed during this study are included in this published article.

Conflicts of Interest

The authors declare no conflicts of interest.

Acknowledgments

The study presented in this paper was supported by Major Science and Technology Projects of Inner Mongolia Autonomous Region (No. zdzx2018029), Technological Innovation Major Project of Hubei Province (Nos. 2019ACA147 and 2019AEE023), and National Key R&D Program of China (No. 2018YFB1600200). This study was also supported by the National Natural Science Foundation of China (No. 71961137010) and Hebei Provincial Communication Department Project (No. YC-201926).

References

[1] X. Dai, Y. Jia, S. Wang, and Y. Gao, "Evaluation of the rutting performance of the field specimen using the Hamburg wheel-tracking test and dynamic modulus test," *Advances in Civil Engineering*, vol. 2020, Article ID 9525179, 15 pages, 2020.

[2] A. Ameli, R. Babago, M. Khabooshani, R. AliAsgari, and F. Jalali, "Permanent deformation performance of binders and stone mastic asphalt mixtures modified by SBS_montmorillonite nanocomposite," *Construction and Building Materials*, vol. 239, Article ID 117700, 2020.

[3] J. Li, J. Yu, J. Xie, and Q. Ye, "Performance Degradation of Large-Sized asphalt mixture specimen under heavy load and its affecting factors using multifunctional pavement material tester," *Materials*, vol. 12, no. 23, p. 3814, 2019.

[4] Y. Xu and L. Sun, "Study on permanent deformation of asphalt mixtures by single penetration repeated shear test," *Procedia - Social and Behavioral Sciences*, vol. 96, pp. 886–893, 2013.

[5] Z. Qasim, A. Abed, and Z. Qasim, "Impact of the Superpavehot mix asphalt properties on its permanent deformationbehavior," in *Proceedings of the 3rd International Conferenceon Buildings, Construction and Environmental Engineering, BCEE3-2017*, Sharm el Sheikh, Egypt, vol. 162, Article ID 01041, 2018.

[6] L. Korkiala-Tanttu and A. Dawson, "Relating full-scale pavement rutting to laboratory permanent deformation testing," *International Journal of Pavement Engineering*, vol. 8, no. 1, pp. 19–28, 2007.

[7] M. Ameri, R. Mohammadi, M. Vamegh, and M. Molayem, "Evaluation the effects of nanoclay on permanent deformation behavior of stone mastic asphalt mixtures," *Construction and Building Materials*, vol. 156, pp. 107–113, 2017.

[8] J. Wang, A. A. A. Molenaar, M. F. C. van de Ven, and S. Wu, "Influence of internal structure on the permanent deformation behavior of a dense asphalt mixture," *Construction and Building Materials*, vol. 171, pp. 850–857, 2018.

[9] Y. Zhao and J. Zhang, "A mechanical model for three-phase permanent deformation of asphalt mixture under repeated load," *Journal of Wuhan University of Technology-Materials Science Edition*, vol. 24, no. 6, pp. 1001–1003, 2019.

[10] F. Zhou, T. Scullion, and L. Sun, "Verification and modeling of three-stage permanent deformation behavior of asphalt mixes," *Journal of Transportation Engineering*, vol. 130, no. 4, pp. 486–494, 2004.

[11] B. Yu, H. Zhu, X. Gu, F. Ni, and R. Guo, "Modified repeated load tri-axial test for the high-temperature performance evaluation of HMA," *Road Materials and Pavement Design*, vol. 16, no. 4, pp. 784–798, 2015.

[12] G. Leonardi, "Finite element analysis for airfield asphalt pavements rutting prediction," *Bulletin of the Polish Academy of Sciences Technical Sciences*, vol. 63, no. 2, pp. 397–403, 2015.

[13] N. Dong, F. Ni, S. Li, J. Jiang, and Z. Zhao, "Characterization of permanent deformation performance of asphalt mixture by multi-sequenced repeated load test," *Construction and Building Materials*, vol. 180, pp. 425–436, 2018.

[14] T. Baghaee Moghaddam, M. Soltani, and M. R. Karim, "Evaluation of permanent deformation characteristics of

unmodified and Polyethylene Terephthalate modified asphalt mixtures using dynamic creep test," *Materials & Design*, vol. 53, pp. 317–324, 2014.

[15] Q. Li, F. Ni, L. Gao, Q. Yuan, and Y. Xiao, "Evaluating the rutting resistance of asphalt mixtures using an advanced repeated load permanent deformation test under field conditions," *Construction and Building Materials*, vol. 61, pp. 241–251, 2014.

[16] H. Fang, Q. Liu, L. Mo, B. Javilla, B. Shu, and S. Wu, "Characterization of three-stage rutting development of asphalt mixtures," *Construction and Building Materials*, vol. 154, pp. 340–348, 2017.

[17] B. Javilla, L. Mo, F. Hao, B. Shu, and S. Wu, "Multi-stress loading effect on rutting performance of asphalt mixtures based on wheel tracking testing," *Construction and Building Materials*, vol. 148, pp. 1–9, 2017.

[18] A. Khodaii, "Mehrara and Evaluation of permanent deformation of unmodified and SBS modified asphalt mixtures using dynamic creep test," *Construction and Building Materials*, vol. 23, no. 7, pp. 2586–2592, 2009.

[19] Q. Guo, L. Li, Y. Cheng, Y. Jiao, and C. Xu, "Laboratory evaluation on performance of diatomite and glass fiber compound modified asphalt mixture," *Materials and Design*, vol. 66, pp. 51–59, 2015.

[20] E. Bocci, "Use of ladle furnace slag as filler in hot asphalt mixtures," *Construction and Building Materials*, vol. 161, pp. 156–164, 2018.

[21] M. Hainin, M. Aziz, Z. Ali et al., "Steel slag as a road construction material," *Jurnal Teknologi*, vol. 73, no. 4, pp. 33–38, 2015.

[22] S. Hasita, R. Rachan, A. Suddeepong et al., "Performance improvement of asphalt concretes using steel slag as a replacement material," *Journal of Materials in Civil Engineering*, vol. 32, no. 8, Article ID 04020227, 2020.

[23] J. Gao, A. Sha, Z. Wang, Z. Tong, and Z. Liu, "Utilization of steel slag as aggregate in asphalt mixtures for microwave deicing," *Journal of Cleaner Production*, vol. 152, pp. 429–442, 2017.

[24] X. Zhou, G. Zhao, S. Tighe et al., "Quantitative comparison of surface and interface adhesive properties of fine aggregate asphalt mixtures composed of basalt, steel slag, and andesite," *Construction and Building Materials*, vol. 246, Article ID 118507, 2020.

[25] L.-A. Esther, L.-G. Pedro, I.-V. Irune, and F. Gerardo, "Comprehensive analysis of the environmental impact of electric arc furnace steel slag on asphalt mixtures," *Journal of Cleaner Production*, vol. 275, Article ID 123121, 2020.

[26] M. Shiha, S. El-Badawy, and A. Gabr, "Modeling and performance evaluation of asphalt mixtures and aggregate bases containing steel slag," *Construction and Building Materials*, vol. 248, Article ID 118710, 2020.

[27] W. Jiao, A. Sha, Z. Liu, W. Jiang, L. Hu, and X. Li, "Utilization of steel slags to produce thermal conductive asphalt concretes for snow melting pavements," *Journal of Cleaner Production*, vol. 261, Article ID 121197, 2020.

[28] H. Goli and M. Latifi, "Evaluation of the effect of moisture on behavior of warm mix asphalt (WMA) mixtures containing recycled asphalt pavement (RAP)," *Construction and Building Materials*, vol. 247, Article ID 118526, 2020.

[29] M. Pasetto, A. Baliello, E. Pasquini, M. Skaf, and V. Ortega-Lopez, "Performance-based characterization of Bituminous Mortars prepared with ladle furnace steel slag," *Sustainability*, vol. 12, no. 5, Article ID 1777, 2020.

[30] W. Liu, H. Li, H. Zhu, and P. Xu, "The interfacial adhesion performance and mechanism of a modified asphalt-steel slag aggregate," *Materials*, vol. 13, no. 5, p. 1180, 2020.

[31] F. Gulisano, J. Crucho, J. Gallego, and L. Picado-Santos, "Microwave healing performance of asphalt mixture containing electric arc furnace (EAF) slag and Graphene nanoplatelets (GNPs)," *Applied Sciences-Basel*, vol. 10, no. 4, p. 1428, 2020.

[32] M. Pasetto and N. Baldo, "Mix design and performance analysis of asphalt concretes with electric arc furnace slag," *Construction and Building Materials*, vol. 25, no. 8, pp. 3458–3468, 2011.

[33] Z. Chen, S. Wu, J. Xie, and J. Chen, "Research on the permanent deformation behavior of asphalt mixture with basic oxygen furnace slag," *Advanced Materials Research*, vol. 689, pp. 304–308, 2013.

[34] M. L. Pattanaik, R. Choudhary, B. Kumar, and A. Kumar, "Mechanical properties of open graded friction course mixtures with different contents of electric arc furnace steel slag as an alternative aggregate from steel industries," *Road Materials and Pavement Design*, vol. 22, no. 2, pp. 268–292, 2019.

[35] GB/T 24175-2009, *Test method stability of steel slag*, People Transportation Press, Beijing, China, 2010.

[36] JTT 1086-2016, *Steel Slag Used in Asphalt Mixture*, People Transportation Press, Beijing, China, 2016.